



Phytochemical Investigations by LC–ESI–MS and Biological Activities of *Arundo Donax* Leaves Extract and Its Silver Nanoparticles

Ahmed M. Al-sayed¹, Nabila H. Shafik*¹, Helana N. Michael¹, Ali A. Ali², F. Abdelhai²
Tamer I.M. Ragab³



¹Chemistry of Tanning Materials and Leather Technology Department, National Research Centre, Dokki, Cairo, Egypt

²Chemistry Department, Faculty of Science, Al-Azhar University, Nasr City 11884, Cairo, Egypt

³Chemistry of Natural and Microbial Products Department, National Research Centre, Dokki, 12622 Cairo, Egypt

Abstract

Arundo donax (Family Poaceae) 70% ethanolic extract was subjected to phytochemical analysis, which revealed the existence of 16 natural flavonoid compounds. Most of these compounds were extracted and characterized using chromatographic methods, chemical degradation, and spectral data (¹H NMR, ¹³C NMR and LC-ESI-MS). This ethanolic extract and its nanoparticles are employed in the assessment of their biological activity. The *A. donax* ethanolic extract was evaluated for the creation of silver nanoparticles, which gave nanoparticles less than 20 nm. Using DPPH (2,2-diphenyl-1-picrylhydrazyl) as the stable radical method, the antioxidant activity of ethanolic extract and its nano was investigated. The results showed a high radical scavenging activity for *A. donax* ethanolic extract, which has a chelating power inhibition of about 65% more than AgNPs (35%). According to the antimicrobial study's findings, the nano extract of *A. donax* has greater antimicrobial activity than the ethanolic extract against gram-positive bacteria like *Bacillus cereus* and *Staphylococcus aureus*, as well as gram-negative bacteria like *Escherichia coli* and pathogenic yeast like *Candida albicans*. At a concentration of 100 g/ml, their cytotoxic activity against the human cancer cell lines A-431 (skin cancer), PC3 (prostate cell line), HCT-116 (colon cell line), and BJ-1 (normal skin fibroblast) revealed that all of the tested samples had a minimal to non-existent cytotoxic effect on the cancer cell lines, whereas the nano extract had a significant cytotoxic effect.

Keywords: *Arundo donax*, Aerial parts, Polyphenolic compounds, LC–MS analysis, Nano particles, Cytotoxicity, Antioxidant and Antimicrobial activity.

Introduction

Poaceae is a large and nearly abundant family of monocotyledonous flowering plants commonly known as grasses. It comprises grasses from natural grasslands, species grown in lawns and pastures, bamboo, and cogon grass. The latter are typically referred to as "grass," and they consist of about 780 genera and 12,000 species [1]. Its constituents are crucial to humankind's economy, agriculture, and environment, and they are distinguished by the presence of flavonoid and flavone C-glycoside molecules [2]. Members of this family are dispersed throughout Egypt, including the Nile Valley, the Oases, the Mediterranean Sea, and the Egyptian Desert [3, 4]. The Egyptians utilized the leaves of *Arundo donax* (*A. donax*) as liner for underground grain storage as early as 5,000 B.C. Mummies

allegedly had *A. donax* leaves wrapped around them. *A. donax* has recently been commercially grown for the purpose of making reeds for musical instruments. Nearly 5,000 years of commercial cultivation may be dated to this type. *A. donax* has not only been grown for musical instruments but also for horticulture uses like garden fences and trellises [5]. The rhizome, or rootstock, was used to treat dropsy in medicine. Cancer treatment involves boiling a root or rhizome in wine and honey. Additionally, condylomata and breast indurations were treated with *A. donax*. As an antilactagogue, depurative, diaphoretic, diuretic, emollient, hypertensive, and sudorific, the root infusion was also utilized. *A. donax* is also used to treat toothaches, pertussis, cystitis, and as a hemostatic [6–8]. Only flavonolignans, vanillic acid, fatty acids, phytosterols, and protocatechualdehyde

*Corresponding author e-mail nabilashafik@yahoo.com

Receive Date: 04 September 2023, Revise Date: 04 December 2023, Accept Date: 04 December 2023

DOI: [10.21608/EJCHEM.2023.233124.8557](https://doi.org/10.21608/EJCHEM.2023.233124.8557)

©2024 National Information and Documentation Center (NIDOC)

substances were isolated and identified from roots, leaving inadequate information on the chemical composition of *A. donax* aerial parts [9]. Through the isolation and chemical characterization of its polyphenolic contents using various chromatographic techniques. The current study intends to evaluate the chemical composition and biological activities of aerial portions of *A. donax* 70% ethanolic extract (*A. donax* ext.). From it, 22 chemicals (Table 1) were discovered for the first time. By using LC-ESI-MS, ^1H NMR, and ^{13}C NMR, the polar compounds were studied. Four human cancer cell lines A-431, PC3, HCT-116, and BJ-1 were tested for cytotoxicity by the two *A. donax* extracts and its AgNPs against DPPH. In addition to exploring their efficacy against pathogenic yeast (*Candida albicans*), gram-positive bacteria (*Bacillus cereus*, *Staphylococcus aureus*), and gram-negative bacteria (*Escherichia coli*).

Materials and Methods

Aerial parts of *A. donax* was collected from MitGammer (Dakahlia Governorate, Egypt), in September 2019 and authenticated by Dr. Mona M. Marzouk, Department of Phytochemical and Plant Systematics, NRC. A voucher specimen (sn. M3313) was deposited in the Herbarium of NRC (CAIRC, Cairo, Egypt).

Chemicals and instruments

NMR experiments were recorded on a Jeol EX-500 spectroscopy: 500 MHz (^1H NMR), 125 MHz (^{13}C NMR). UV spectrophotometer (Shimadzu UV-240). Column chromatography (CC) Polyamide 6S (Riedel-De-Haen AG, SeelzeHaen AG, SeelzeHanver, Germany) and Sephadex LH-20 (Pharmazia) using EtOH/H₂O or MeOH / H₂O as eluent. Paper chromatography (PC) (descending) Whatman No. 1 and 3 MM papers, using solvent systems 1) H₂O, 2) 15% HOAc, 3) BAW (n-BuOH-HOAc-H₂O 6:1:2). Complete acid hydrolysis (2 N HCl, 2 h, 100 °C) and mild acid hydrolysis (0.1 N HCl, 1 hour, 100 °C) were carried out and followed by paper co-chromatography with authentic samples to identify the aglycones and sugar moieties.

Extraction and isolation

Aerial parts of *A. donax* plant was freshly collected and washed with distilled water and then, dried in a shade at room temperature for 7 day. The dried aerial part was milled using high speed blender (IKA, Laboratechnic, Germany). The milled powder (3 Kg) were subjected to the extraction process using 70% (v/v) aqueous ethanol overnight for three successive times. The reaction mixture was filtered and dried using a Rotavapour[®]. The extract was defatted by using petroleum ether (40–60 °C). The defatted extract was slurred with water and then, mixed with a

small amount of polyamide and subjected to a polyamide CC, starting with water as eluent then decreasing the polarity by increasing the concentration of ethanol up to 100%. 10 fractions were obtained and grouped based on their paper chromatography properties using 15% AcOH, and BAW (n-BuOH-HOAc-H₂O 6:1:2) as eluents, respectively. PPC was carried out for isolation and purification of the flavonoid compounds. All glass chromatography tanks were used applying the paper descending techniques. The developed chromatograms were air-dried and examined before spraying in both visible and UV light. The chromatograms were exposed to ammonia vapors, then immediately reexamined to observe changes in colors or fluorescence under UV light. Finally, ten fractions were collected, dried and subjected to repeated purification on columns of Sephadex LH-20 to give the isolated compounds. Identification of the isolated compounds were carried out through R_f -values, colour reactions, chemical investigations (complete and mild acid hydrolysis) and physical investigations (UV, NMR, ESI-MS and LC-QTOF-HR-MS/MS).

Chemical data for some isolated compounds

Luteolin-6-C-glucoside (1) was obtained as an amorphous yellow powder eluted with 80% EtOH from a polyamide column. It appeared as a dark purple spot on the PC under UV light, turned yellowish green upon exposure to ammonia vapours, and then turned dirty green after spraying with a 1% methanol ferric chloride solution. UV/Vis λ_{max} (nm) MeOH: 256, 270sh, 350; The NaOMe: 265, 275sh, 405; AlCl₃: 276, 302sh, 330, 423; AlCl₃/HCl: 266*, 278, 365, 382; NaOAc: 275, 321, 390; NaOAc/H₃BO₃: 264, 370, 425*. R_f = 37 (6% AcOH) and 44 (BAW). ^1H -NMR (500 MHz, DMSO-*d*₆), Aglycone moiety: δ (ppm): 7.38 (1H, dd, J = 2.5 Hz, 9.0 Hz, 6'-H), 7.38 (1H, d, J = 2.5 Hz, 2'-H), 6.89 (1H, d, J = 9.0 Hz, 5'-H), 6.52 (1H, s, 3-H), Sugar moiety: 4.45 (1H, d, J = 10.0 Hz, 1''-H). ^{13}C -NMR (125 MHz, DMSO-*d*₆), Aglycone moiety: δ (ppm): 163.45 (C-2), 103.75 (C-3), 182.54 (C-4), 160.57 (C-5), 107.72 (C-6), 164.79 (C-7), 93.76 (C-8), 157.24 (C-9), 102.46 (C-10) 121.56 (C-1'), 112.92 (C-2'), 145.50 (C-3'), 149.50 (C-4'), 115.35 (C-5'), 118.88 (C-6'), Sugar moiety: 81.18 (C-1''), 70.36 (C-2''), 73.86 (C-3''), 71.16 (C-4''), 78.69 (C-5''), 61.44 (C-6'').

Isorhamnetin-3-O-rutinoside (2) was obtained as Yellow powder appeared as a Brown spot on the PC under UV light convert to yellow with ammonia, isolated with 60% EtOH, R_f values 45 in BAW and 61 in 15% AcOH, UV λ_{MeOH} max nm: 255, 271sh, 322sh, 367; NaOMe 272, 328, 418; AlCl₃ 268, 303sh, 362, 403; AlCl₃-HCl 270, 300sh, 358, 403;

NaOAc 280, 328sh, 400; NaOAc-H₃BO₃ 255, 270sh, 303sh, 360. ¹H-NMR (500 MHz, DMSO-*d*₆) Aglycone moiety: δ (ppm) δ: 7.84 (1H, d, *J* = 1.70 Hz, H-2'), 7.50 (1H, dd, *J* = 8.0, 1.70 Hz, H-6'), 6.90 (1H, d, *J* = 8.4 Hz, H-5'), 6.40 (1H, d, *J* = 1.6 Hz, H-8), 6.18 (1H, d, *J* = 1.6 Hz, H-6), 3.82 (3H, s, OCH₃-3'). Sugar moiety: 5.42 (d, *J* = 7.45 Hz, glc-H-1''), 4.40 (1H, s, H-1''' of anomeric proton of rhamnose), 0.96 (d, *J* = 6.3 Hz, rhamnosyl methyl group), 3.2-3.9 (m, sugar protons);). ¹³C-NMR (125 MHz, DMSO-*d*₆) Aglycone moiety: δ (ppm): 157.3 (C-2), 133.58 (C-3), 177.3 (C-4), 161.6 (C-5), 99.3 (C-6), 164.6 (C-7), 94.5 (C-8), 157.1 (C-9), 104.6 (C-10), 121.6 (C-1'), 113.7 (C-2'), 147.4 (C-3'), 149.8 (C-4'), 115.8 (C-5'), 122.4 (C-6'), 56.29 OCH₃. Sugar moiety: Glucose sugar at δ (ppm): 101.7 (C-1''), 74.7 (C-2''), 76.8 (C-3''), 70.7 (C-4''), 76.3 (C-5''), 67.5 (C-6''). Rhamnose sugar at: δ (ppm): 101.4 (C-1'''), 70.8 (C-2'''), 71.1 (C-3'''), 72.3 (C-4'''), 68.8 (C-5'''), 18.1 CH₃ of Rhamnose.

Kaempferol 3-O-neohesperidoside (3) yellow powder, dark spot on paper chromatography convert to bright yellow with ammonia and aluminium chloride which eluted with 40% EtOH from polyamide CC, R_f values 28 in BAW and 80 in 15% AcOH, UV/Vis λ_{max} (nm) MeOH(a): 267, 295*, 353., NaOMe: 273, 328*, 405., NaOAc (b): 273, 300*, 370., H₃BO₃: 267, 295*, 353., AlCl₃ (c): 274, 300*, 348*, 398., HCl: 274, 300*, 345*, 399. ¹H-NMR (500 MHz, CD₃OD) δH (ppm): 6.15 (1H, brs, H-6), 6.35 (1H, brs, H-8), 8.02 (2H, d, *J* = 8.4 Hz, H-2', 6'), 6.87 (2H, d, *J* = 8.4 Hz, H-3', 5'), Glc: 5.72 (1H, d, *J* = 7.6 Hz, H-1''), 3.60 (1H, dd, *J* = 7.6, 9.0 Hz, H-2''), 3.53 (1H, t, *J* = 9.0 Hz, H-3''), 3.27 (1H, t, *J* = 9.0 Hz, H-4''), 3.22 (1H, m, H-5''), 3.48 (1H, dd, *J* = 12.0, 5.0 Hz, H-6''), 3.71 (1H, dd, *J* = 12.0, 1.5 Hz, H-6''), Rham: 5.21 (1H, d, *J* = 1.6 Hz, H-1'''), 3.98 (1H, dd, *J* = 3.0, 1.6 Hz, H-2'''), 3.75 (1H, dd, *J* = 9.0, 3.0 Hz, H-3'''), 3.31 (1H, t, *J* = 9.0 Hz, H-4'''), 4.00 (1H, m, H-5'''), 0.93 (3H, d, *J* = 6.0 Hz, H-6'''). ¹³C-NMR (125 MHz, DMSO-*d*₆) Aglycone moiety: δ (ppm): 161.3 (C-2), 134.4 (C-3), 179.3 (C-4), 163.2 (C-5), 99.7 (C-6), 165.9 (C-7), 94.6 (C-8), 158.4 (C-9), 105.9 (C-10), 123.1 (C-1'), 132.1 (C-2'), 116.2 (C-3'), 148.4 (C-4'), 116.2 (C-5'), 132.1 (C-6'). Sugar moiety: Glucose sugar at δ (ppm): 100.2 (C-1''), 80.0 (C-2''), 78.9 (C-3''), 71.8 (C-4''), 78.4 (C-5''), 62.0 (C-6''). Rhamnose sugar at: δ (ppm): 102.6 (C-1'''), 72.4 (C-2'''), 72.3 (C-3'''), 74.4 (C-4'''), 69.6 (C-5'''), 17.5 CH₃ of Rhamnose

Hesperitin (4) was obtained as an amorphous yellow powder, which appeared as a dark purple spot on the PC under UV light and turned yellowish green upon exposure to ammonia vapors and then turned dirty green after spraying with 1% methanol ferric chloride, eluted with 100 % EtOH from polyamide CC. Its R_f value=37 (6% AcOH) and 44 (BAW). ¹H-

NMR (500 MHz, DMSO-*d*₆) δ (ppm) 6.95 (d, *J* = 1.6 Hz H-2' and 6.90 (dd, *J* = 8.2, 1.6 Hz H-6'); 6.95 (d, *J* = 8.2 Hz H-5'); 5.92 (d, *J* = 1.6 Hz, H-8); 5.91 (d, *J* = 1.9 Hz, H-6). 3.81 (s, OCH₃-4'). ¹³C-NMR (125 MHz, DMSO-*d*₆) δ (ppm) 79.6 (C-2), 43.4 (C-3), 196.4 (C-4), 165.2 (C-5), 97.3 (C-6), 168.6 (C-7), 96.2 (C-8), 102.9 (C-9), 164 (C-10), 123.3 (C-1'), 129.4 (C-2'), 114.1 (C-3'), 160.6 (C-4'), 114.1 (C-5'), 129.4 (C-6'), 55.9 (OCH₃-3').

LC–ESI–MS analysis

Fragmentation analyses were performed using (Triple TOF 5600+). The mobile phases consisted of DI-Water containing 0.1% FA (formic acid), ammonium format buffer pH=8 containing 1% methanol and 100 % acetonitrile, in-Line filter discs Pre column (0.5 μm x 3.0 mm, Phenomenex), X bridge C18 column (3.5 μm, 2.1x50 mm, waters) and the column temperature was maintained at 40°C, flow rate 0.3 ml/min and the scan type (Information Dependent Acquisition (IDA)). *A. donax ext.* were defatted and desalted by CHCl₃ and, respectively, by warming under reflux conditions. The mobile phase working solution (MP-WS) was prepared from DI-Water-Methanol-Acetonitrile (50: 25: 25 v/v). Add 1 ml of MP-WS to 50 mg weighted sample, vortex for 2 min followed by ultra-sonication for 10 min, and centrifuge for 5 min at 10000 rpm. An amount of 20 μl stock (50/ 1000 μl) was diluted with 1000 μl reconstitution solvent. Finally, the injected concentration was 1 μg/μl. Inject 25 μl from the total extract on positive mode and 25 μl MP-WS as a blank sample. Master View was used for feature peaks extraction from the total ion chromatogram (TIC) based on features that should have Signal-to-Noise greater than 5 (Non-targeted analysis). Features intensities of the sample-to-blank should be greater than 5. Marker View was used for feature annotation and removing isotopic peaks. Master View was used again to identify peaks based on their fragments using Built-in database and online database; RESPECT and MONA (Mass Bank of North America).

Green synthesis of silver nanoparticles

The obtained extract was dried, powdered, and stored. An aqueous solution of 1 mM silver nitrate (AgNO₃) was prepared in a 250 ml Erlenmeyer flask and used for the synthesis of AgNPs. Briefly, three different conc. of *A. donax ext.* were prepared and added to an aqueous solution of 1 mM silver nitrate and incubated in the dark overnight at room temperature. The complete reduction of AgNO₃ to Ag⁺ ions was confirmed by the change in color from colorless to colloidal brownish yellow. The colloidal mixture was then sealed and stored properly for future use. The formation of AgNPs was further confirmed by spectrophotometric analysis [10].

DPPH assay

The antioxidant capacity of the *A. donax. ext.* and Ag NPs. of *A. donax* was measured using a DPPH method described by using the free radical 2,2-diphenyl-picrylhydrazyl (DPPH). Aliquots (0.1 mL) of diluted extracts in methanol were added to 1 mL of DPPH solution and the absorbance of the DPPH solution was determined at 517 nm after 30 min of incubation at room temperature. Appropriate blanks (methanol) and standard (Trolox solution in methanol) were used to compare the antioxidant capacity of *A. donax ext.* All measurements were done in triplicate. The radical-scavenging activity (RSA) was calculated as a percentage of DPPH discoloration using the equation 1 [11].

$$\% \text{ RSA} = (A_{\text{blank}} - A_{\text{sample}} / A_{\text{blank}}) \times 100$$

(Equation 1)

Cell culture

A431 skin cancer and prostate cancer (PC3) were maintained in DMEM medium, and HCT-116 colorectal carcinoma, BJ1 normal skin fibroblast were maintained in RPMI. All media were supplemented with 10% foetal bovine serum and incubated at 37 °C in 5% CO₂ and 95% humidity. Cells were subcultured using trypsin versene 0.15%. All cell lines were purchased from Vacsera (Giza, Egypt).

Cytotoxic effect on human cell lines

Cell viability was assessed by the mitochondrial-dependent reduction of yellow MTT (3-(4,5-dimethylthiazol-2-yl)-2,5-diphenyl tetrazolium bromide) to purple formazan [12]. Procedure: All the following procedures were done in a sterile area using a Laminar flow cabinet biosafety class II level (Baker, SG403INT, Sanford, ME, USA). Cells were suspended in DMEM-F12 medium [(for A431 (skin cancer), PC3 (prostate cell line), HCT116 (colon cell line)] beside one normal cell line (BJ1), 1% antibiotic-antimycotic mixture (10,000U/ml Potassium Penicillin, 10,000µg/ml Streptomycin Sulphate and 25µg/ml Amphotericin B) and 1% L-glutamine at 37 °C under 5% CO₂. Cells were batch cultured for 10 days, then seeded at a concentration of 10x10³ cells/well in fresh complete growth medium in 96-well microtiter plastic plates at 37 °C for 24 h under 5% CO₂ using a water-jacketed Carbon dioxide incubator (Sheldon, TC2323, Cornelius, OR, USA). Media was aspirated, fresh medium (without serum) was added and cells were incubated either alone (negative control) or with different concentrations of sample to give a final concentration of (100-50-25-12.5-6.25-3.125-0.78 and 1.56 ug/ml). After 48 h of incubation, the medium was aspirated, 40ul MTT salt (2.5µg/ml) was added to each well and incubated for further four

hours at 37°C under 5% CO₂. To stop the reaction and dissolve the formed crystals, 200µL of 10% Sodium dodecyl sulphate (SDS) in deionized water was added to each well and incubated overnight at 37°C. A positive control composed of 100µg/ml was used as a known cytotoxic natural agent that gives 100% lethality under the same conditions [12]. The absorbance was then measured using a microplate multi-well reader (Bio-Rad Laboratories Inc., model 3350, Hercules, California, USA) at 595nm and a reference wavelength of 620nm. A statistical significance was tested between samples and negative control (cells with the vehicle) using an independent t-test by SPSS 11 program. DMSO is the vehicle used for the dissolution of plant extracts and its final concentration in the cells was less than 0.2%. The percentage of change in viability was calculated according to the formula (Equation 2):

$$((\text{Reading of extract} / \text{Reading of negative control}) - 1) \times 100 \text{ (Equation 2)}$$

A probit analysis was carried out for IC₅₀ and IC₉₀ determination using SPSS 11 program. In the present study, the degree of selectivity of the synthetic compounds is expressed as SI=IC₅₀ of the pure compound in a normal cell line/IC₅₀ of the same pure compound in a cancer cell line, where IC₅₀ is the concentration required to kill 50% of the cell population.

Antimicrobial Activity

Qualitative evaluations were carried out in nutrient broth according to [13-14]. The inoculation of pathogenic microorganisms used in this study were Gramme-positive bacteria (*Bacillus cereus* & *Staphylococcus aureus*), Gramme-negative bacteria (*Escherichia coli* & *Pseudomonas aeruginosa*), and pathogenic yeast (*Candida albicans*), was prepared from fresh overnight broth cultures using nutrient broth medium that were incubated at 37°C [15]. The inoculum size of this pathogenic strain was prepared and adjusted to approximately 0.5 McFarland standard (1.5 × 10⁸ CFU /ml) [15], and 25.0 µL inoculum size of each microorganism strain was separately inoculated into each plate containing 20.0 ml of the sterile nutrient agar medium (NA). The samples were applied After the media cooled and solidified on a 0.9 cm well of that inoculated agar plates which were prepared previously by using a 1.0 cm cork borer applying the Well Diffusion Method, in this method each well was filled with 100.0 µl of each sample separately [15].

Results and Discussion

Phenolics investigation LC-QTOF-HR-MS/MS of polyphenolic compounds

LC-QTOF-HR-MS/MS was used in the current investigation to identify the polyphenolic 2RY metabolites in *A. donax* ethanol extract. The limit of detection for each peak of chemicals was calculated using the RT, full MS spectra, and MS². Literature and reference compound spectra were compared to identify fragmentation patterns in the negative mode as shown in Fig. (1). 22 potential compounds were tentatively identified in *A. donax* extract and characterized in (Table 1) as phenolic acids, quinic acids and derivatives (1), chlorogenic acid (5), and rosmarinic acid (3). Flavonoids: myricetin (4). Isosakuranetin-7-O-neohesperidoside (7), Luteolin-3', 7-di-O-glucoside (8), Kaempferol-3-O-(6'-p-coumaroyl)-glucoside (9), Kaempferol-7-neohesperidoside (10), Luteolin-6-C glucoside (11), Isorhamnetin-3-O-rutinoside (12), Okanin-4'-O-glucoside (13) Kaempferol-3-O-glucuronouide (14), Apigenin 8-C-glucoside (15), Daidzein-8-Cglucoside (16), Luteolin (18), 3, 5, 7-trihydroxy-4'-methoxyflavone (Diosmetin) (19), isorhamnetin-3-O-glucoside (20), Hesperetin (21), Apigenin (22), Coumarin; Esculine (17).

Phenolic acids are a class of secondary metabolites (SM) that have a variety of interesting biochemical pathways. They usually form a pseudomolecular ion [M-H]⁻ corresponding to a deprotonated molecule and characteristic fragment ion [M-H-44] related to CO₂ loss from the carboxylic acid group. In this work, three free phenolic acids were tentatively identified, including, quinic acid, chlorogenic acid and rosmarinic acid depending on a molecular ion peak at m/z 191.0192, 353.0877 and 359.1121.

There were found to be four flavonoid diglycosides in *A. donax*. Extract comparable to Isosakuranetin-7-O-neohesperidoside, Luteolin-3', 7-di-glucoside and Kaempferol-7-neohesperidoside, Isorhamnetin-3-O-rutinoside and (peaks 7, 8, 9 and 10).

Peak 7 displayed a molecular ion peak at m/z 593.2551 as well as unique fragment ions at m/z 447.0835[M-H-146]⁻, 285.0331[M-H-(146+162)]⁻. due to the loss of rhamnose and glucose units, respectively.

Peak 8 showed a molecular ion peak at m/z 609.1456 and specific fragment ions at m/z 327.04819, 357.02969, 447.08875[M-H-162]⁻ and 489.0929[M-H-120]⁻ due to the loss of di glucose sugar units, respectively.

Peak 9 displayed a molecular ion peak at m/z 593.1496 and distinctive fragment ions at m/z 327.05878, 429.08008, 447.10104 [M-H-146]⁻ and 473.11649[M-H-120]⁻ due to the loss of rhamnose and glucose units, respectively.

Peak 10 showed a signal for a molecular ion at m/z 623.1681 and distinctive fragment ions at m/z 473.0970, 477.04791[M-H-146]⁻, 315.09321[M-H-(146+162)]⁻, 255.04561, 257.0092 due to the loss of rhamnose and glucose units, respectively.

Five flavonoid monoglycosides were detected by LC-Q-TOF- HR-MS/MS analysis in *A. donax. ext.* corresponding to Isorhamnetin-3-O-glucoside, Luteolin-6-C-glucoside, Kaempferol-3-glucuronide, apigenin 8-glucoside and apigenin 6-glucoside (peaks 11, 12, 15, 16 and 17).

Peak 11 originated from isorhamnetin aglycone based on the characteristic deprotonated fragment at m/z 315.05316[M-H -162]⁻ and product ions at m/z 179.002 and 151.9352 so peak 10 established as Isorhamnetin-3-O-glucoside due to loss of glucose moiety. peak 12 produced [M-H]⁻ at m/z 447.094 and showed predominant ions at m/z 285.04535[M-H -162]⁻, 327.04788 [M-H-120]⁻, 357.06403[M-H-90]⁻ so peak 12 tentatively identified as Luteolin-6-C-glucoside.

Peak 15 was tentatively characterized as Kaempferol-3-glucuronide based on its molecular ion peak at m/z 461.1086 and intensive product ions at m/z 285.2497, 309.04062. Two derivatives of apigenin at the same molecular ion peak m/z 431 were tentatively established based on their intensive fragment at m/z 311[M-H-120]⁻, 341.06851 [M-H-90]⁻ and different retention time which indicated that they were derived from apigenin aglycone. They were tentatively identified as apigenin 8-glucoside and apigenin 6-glucoside, respectively Peak (16, 17).

In the QTOF-MS/MS analysis two flavanone compounds were tentatively identified and assigned as hesperetin (peak 21) at m/z 301.0707 and Isosakuranetin-7-O-neohesperidoside (peak 6) at m/z 593.2551.

One Isoflavone component was assigned at m/z 415.1603 and identified as Daidzein-8-C-glucoside peak 18 as in table 1 due to loss of hexose moiety based on the characteristic fragments at m/z 325.1066[M-H-90]⁻, 295.11032[M-H-120]⁻, 255.3201 and 199.14822.

Peaks (4, 20 and 23) showing a [M-H]⁻ ions at m/z 317.0562, 285.0412 and 269.0427; MS₂ ions at m/z 180.00751, 116.0583, 248.97894 for myricetin, 133.02901, 151.00749, 199.03011 for luteolin and 159.99678; 225.05598 for apigenin.

One Coumarin glycosides was detected for the first time in *A. donax. ext.* Based on MS/MS analysis as Esculin, peak 19 as in table [1].

Green syntheses of silver nanoparticles UV-visible spectra

Studies using UV-vis spectroscopy Brilliant colours are a defining characteristic of Ag nanoparticle dispersions. Surface plasmon resonance (SPR) in the reaction mixture, which causes the reaction mixture to appear brownish-yellow, has been interpreted as proof that Ag nanoparticles have formed [16]. The UV-vis spectra of the Ag nanoparticles produced when three different doses of *A. donax* were added to 10 mL of 10⁻³ M AgNO₃

solution are shown in Fig. (2). The SPR band causes an absorption in the visible area of the samples in their as-prepared state between 485 and 495 nm. The gradual addition of *A. donax* ext. increases the SPR band's intensity. As the SPR band gets stronger, it means that more Ag^+ ions are being converted into Ag nanoparticles.

A high number of functional groups are now available for the reduction and capping of the Ag nanoparticles as a result of the extract's enhanced concentration. The optimal concentration of *A. donax* extract at which nanoparticles are stabilized is 300, as depicted in Fig. 2 [10].

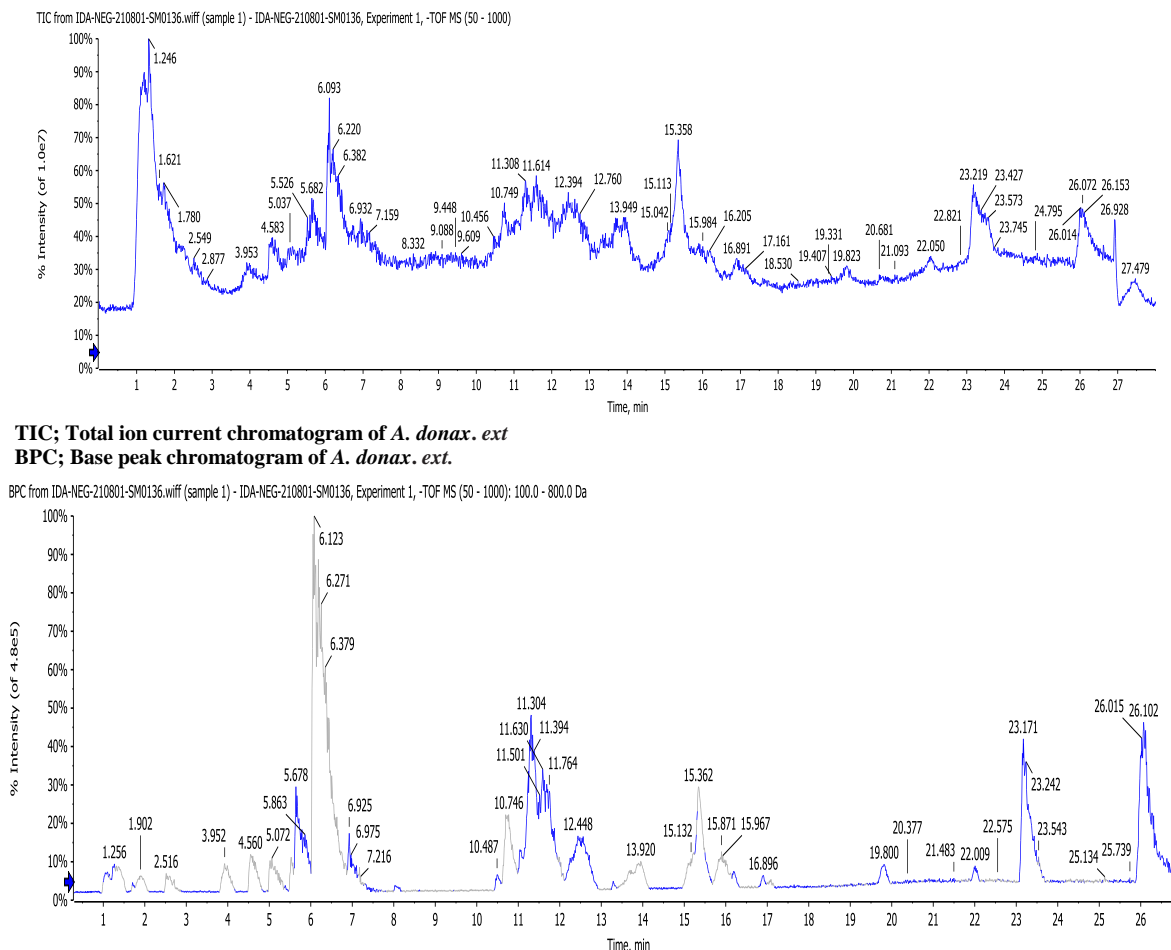


Figure [1]: Negative-MODE – TIC and BPC of *A. donax* extract

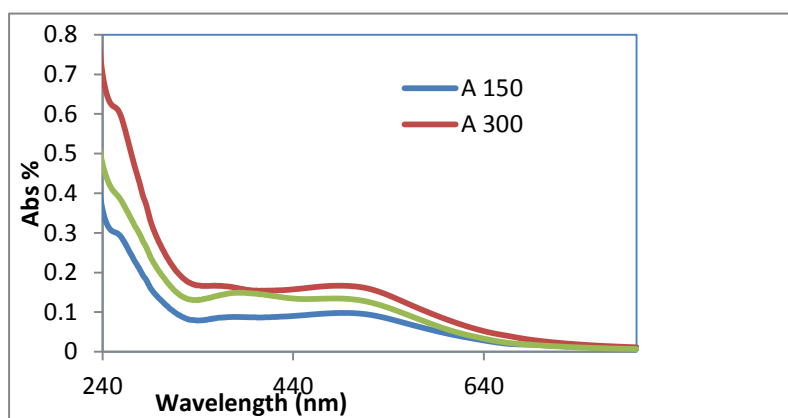


Fig [2]: Ag nanoparticles' SPR band was observed in UV-vis spectra as a result of various *A. donax* extract additions.

Table [1]: LC-ESI-MS analysis of phenolic compounds of *A. donax* extract

Peak No	Tentatively compounds	identif RT min.	[M-H] ⁻ m/z	Error(ppm)	Formula	Classes	MS/MS m/z	Ref.
1	D-(-)-Quinic acid	1.035167	191.0192	-0.8	C ₇ H ₁₂ O ₆	Quinic acids and derivatives	109.02979, 173.00858	16
2	D-(-)-Quinic acid	1.164333	191.0543	4.7	C ₇ H ₁₂ O ₆	Quinic acids and derivatives	173.03998,	16
3	Rosmarinic acid	1.40518	359.1121	-2.4	C ₁₈ H ₁₆ O ₈	Coumaric acids and derivatives	133.04222, 179.91898	17
4	Myricetin	1.177	317.0562	-0.8	C ₁₅ H ₁₀ O ₈	Flavonols	180.00751, 248.97894	18
5	Chlorogenic acid	2.330767	353.0877	-1	C ₁₆ H ₁₈ O ₉	Quinic acids and derivatives	173.04256, 191.05885	19
6	L-(-)-Phenylalanine	2.433433	164.0334	5.4	C ₉ H ₁₁ NO ₂	Phenylalanine and derivatives	118.02936, 120.04315, 149.04384	20
7	Isosakuranetin-7-O-neohesperidoside	4.15080	593.2551	12.1	C ₂₈ H ₃₄ O ₁₄	Flavonoid-7-O-glycosides	433.98487, 187.13893:5	21
8	Luteolin-3',7-di-O-glucoside	5.022666	609.1456	0.8	C ₂₇ H ₃₀ O ₁₆	Flavonoid-7-O-glycosides	327.04819,357.02969, 447.08875, 489.0929	22
9	Kaempferol-7-neohesperidoside	5.524017	593.1496	0.6	C ₂₇ H ₃₀ O ₁₅	Flavonoid-7-O-glycosides	327.05878,429.08008, 447.10104, 473.11649	19
10	Isorhamnetin-3-O-rutinoside	5.908916	623.1681	-5.6	C ₂₈ H ₃₂ O ₁₆	Flavonoid-3-O-glycosides	473.0970, 447.04791, 284.09321, 255.04561, 257.0092	17
11	Isorhamnetin-3-O-glucoside	9.5665	477.1048	48.8	C ₂₂ H ₂₂ O ₁₂	Flavonoid-3-O-glycosides	179.002, 151.9352,315.05316	30
12	Luteolin-6-C-glucoside	5.666934	447.094	-0.3	C ₂₁ H ₂₀ O ₁₁	Flavonoid glycosides	C- 284.04535, 357.06403	23
13	Kaempferol-3-O-(6 ^o -p-coumaroyl)-glucoside	5.524017	593.1221	46.9	C ₃₀ H ₂₆ O ₁₃	Flavonoid-3-O-p-coumaroyl glycosides	309.04785:	19
14	Okanin-4'-O-glucoside	6.006083	449.1481	0.2	C ₂₁ H ₂₂ O ₁₁	Flavonoid-O-glycosides	287.04279	24
15	Kaempferol-3-Glucuronide	6.081817	461.1086	0.2	C ₂₁ H ₁₈ O ₁₂	Flavonoid-3-O-glucuronides	309.04062	25
16	Apigenin 8-C-glucoside	6.205733	431.1025	-6.4	C ₂₁ H ₂₀ O ₁₀	Flavonoid glycosides	8-C- 311.06659, 431.08865	26
17	Apigenin 6-C-glucoside	6.385733	431.1026	-6.7	C ₂₁ H ₂₀ O ₁₀	Flavonoid-8-C-glycosides	311.05701, 341.06851	26
18	Daidzein-8-C-glucoside	7.5163	415.1603	-8.2	C ₂₁ H ₂₀ O ₉	Isoflavonoid-C-glycosides	137.1066, 255.11032 199.14822	26
19	Esculin	8.98825	339.1258	-2.8	C ₁₅ H ₁₆ O ₉	Coumarin glycosides	149.06668, 139.10648	177.09677, 27
20	Luteolin	9.4484	285.0412	-0.9	C ₁₅ H ₁₀ O ₆	Flavones	133.02901, 199.03011	151.00749, 28
21	3, 5, 7-trihydroxy-4'-methoxyflavone (Diosmetin)	9.473733	315.0544	-8.6	C ₁₆ H ₁₂ O ₆	Diosmetin	179.8223, 151.03941	29
22	Hesperetin	10.34152	301.0707	1.8	C ₁₆ H ₁₄ O ₆	4'-O-methylated flavonoids	255.23303, 131.07016:250	19
23	Apigenin	10.55000	269.0472	-3.6	C ₁₅ H ₁₀ O ₅	Flavones	117.03425,159.99678: 225.05598,	19

HRTEM analysis

HRTEM images of synthesized silver nanoparticles using *A. donax* ext. at room temperature. The TEM pictures displayed below in Fig. 3 at various magnifications demonstrate that the Ag NP forms are spherical in shape and that the particle sizes range from 3 to 20 nm [31].

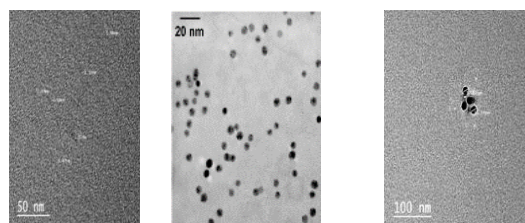


Fig. [3]: The TEM images of the Ag NPs synthesised using *A. donax* extract

FT-IR spectroscopy

A. donax ext. aerial portions have a variety of phytochemicals in them, including saponins, flavonoids, C-glycosides, plant sterols, polysaccharides, and tannins. These phytochemicals include lots of amino and hydroxyl groups. The presence of such functional groups was cited in several papers as the cause of the decrease in metal nanoparticles [32, 33]. Therefore, FTIR is a sensitive method for identifying the functional groups in charge of reducing Ag nanoparticles. The FTIR spectra of the Ag nanoparticles stabilized by *A. donax* are shown in Figure 4 alongside those of the raw extract. The range of *A. donax* ext. IR peak spreads widely across the spectral area (3600-3000 cm^{-1}) in its spectrum. The stretching vibrations of the -OH, NH, and CH groups are responsible for the IR bands in this area [34]. The (-OH) group was attributed to the IR signal at 3342 cm^{-1} , whereas the (-NH) amino group found in proteins was responsible for the signal at 3104 cm^{-1} [13]. A large IR peak owing to the in-plane bending of the (-OH) group of phenol or tertiary alcohol was discovered at 1523 cm^{-1} , while the bending vibrational peak of the (-NH) group was identified at 1747 cm^{-1} . It has been discovered that the stretching vibration of (-C-N) aromatic and aliphatic amines occurs in the IR band at 1060 cm^{-1} . Four further noteworthy modifications to the FTIR spectra were observed after interaction with AgNO_3 . First, the amino group's band was moved to 3342 cm^{-1} while the (-OH) band was sharpened and transferred to 3540 cm^{-1} . Second, at 1751 cm^{-1} , the (-NH) bending was moved to the side with higher energy. Third, the (-C-O) bending was claimed to be the cause of the new peak's development at 1392 cm^{-1} [35, 36]. The fourth change was an increase in the (-C-N) stretching vibration and a minor shift to 1126 cm^{-1} . According to these spectroscopic findings, the phytochemicals in *A. donax* ext. contain hydroxyl and amino groups, which are responsible for their reducing potential. The silver metal vibrations are what caused the peak at 1126 cm^{-1} as in Fig. 4. One property of flavanones is their adsorption on the surface of silver metal nanoparticles. Stretching vibrations of the phenolic or carboxylic groups contained in the extract cause all of these conspicuous peaks, which are proteins and flavanones found in synthesized Ag NPs. So it stands to reason that these biomolecules are in charge of capping and effectively stabilizing synthesized nanoparticles.

Cytotoxic activity

Antitumor medications made from plant components are becoming more popular due to the increased interest in finding a treatment for tumors and their minimal side effects. *A. donax*'s anticancer activity

has only been briefly discussed in publications up to this point [37]. As a result, the cytotoxicity of *A. donax* and its Ag NPs was assessed against the skin cancer cell lines A431 and HCT-116 as well as the normal skin fibroblast BJ-1. First, extracts were applied to cultures of different cell lines at a concentration of 100 $\mu\text{g/ml}$. The cytotoxic effect was investigated (Table 2). In contrast to the nano extract, which exhibited a strong cytotoxic effect against A-431 and PC3 (90.7% and 95.3%, respectively), all of the *A. donax* extract samples examined had a weak to nonexistent effect on all of the cancer cells tested. *Arundodonax* was coupled with *Cynodondactylon L.* and *Spartiumjunceum L.* for the treatment of malignancies [37].

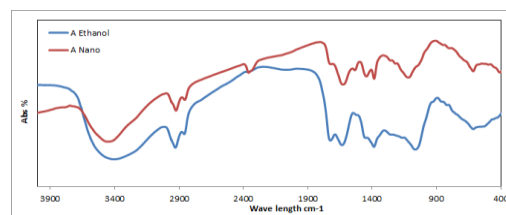


Fig. [4]: (FTIR) of *A. donax* ext. and AgNPs. of *A. donax*

Table 2: Cytotoxicity of *A. donax* ext. and of at 100 $\mu\text{g/ml}$ on three human tumor cell lines and one normal cell line.

Sample	Cytotoxic activity % at 100 ($\mu\text{g/ml}$)			
	A431	PC3	HCT116	BJ1
<i>A. donax</i> ext.	13.6	22	23.6	3.2
<i>A. donax</i> AgNPs	90.7	95.3	38.2	26.6

For the most active, which showed a high cytotoxic effect of the tested cancer cell line, more than 75% of dose responses were studied at different concentrations of 100-50-25-12.5-6.25-3.125-1.56 and 0.78 $\mu\text{g/ml}$. to calculate the IC_{50} value (Table 3). Positive control: Adrinamycin (doxorubicin) [Mw = 579.99]

Table [3]: IC_{50} ($\mu\text{g/ml}$) against A431 and PC3

Sample	IC_{50} value ($\mu\text{g/ml}$)	
	A431	PC3
AgNPs of <i>A. donax</i> .	33.3	32.6
Doxorubicin	24.9	26.1

A431 (skin cancer), PC3 (prostate cell line), BJ1 (normal skin fibroblast), HCT116 (colon cell line)

DPPH activity

The radical scavenging activity of *A. donax* ext. and AgNPs of *A. donax* were tested using the 'stable' free radical (DPPH) (Table 4). Which *A.*

donax have Chelating power Inhibition about 65 % more than AgNPs of 35 % and its logic according to the principle of free radical mechanism. In terms of the importance of antioxidant activity due to its great importance in the prevention of cancer. The antioxidant activity of *A. donax* and AgNPs were evaluated. The results showed that the conversion of *A. donax* ext. to AgNPs form resulted in 37% reduction of antioxidant activity in comparison to *A. donax* ext. Also, as it was seen in Fig. 5 the antioxidant activity of *A. donax* ext. (67%) is near to the vitamin C (81%). This result could be back to the liberation of the Flavonoids and phenolic during the nanoparticle formation process and these chemicals are responsible for plants' antioxidant activity [38,39].

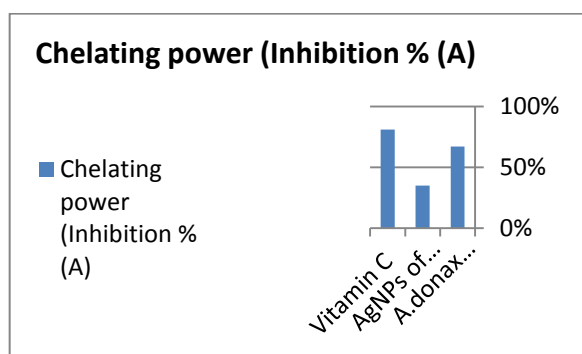


Fig. [5]: Free Free radical scavenging activity of *A. donax* and AgNPs of *A. donax* using DPPH assay at concentration of 100 ($\mu\text{g/ml}$)

Table [4]: Free radical scavenging activity of samples using DPPH assay at concentration of 100 ($\mu\text{g/ml}$)

Extracts	Chelating Inhibition % (A)	power
<i>A. donax</i> ext.	67 %	
AgNPs of <i>A. donax</i>	35 %	
Vitamin C	81 %	

Antimicrobial activity

The results in Table 5 showed that the conversion of *A. donax* ext. to nanoparticle form had a noticeable effect on the antimicrobial activity, with a degree of variation depending on the strain type. For instance, the AgNPs form could inhibit *Staphylococcus aureus* (18mm) and *Bacillus cereus* (16mm) in comparison to 11mm for both of the native extracts. This result could be attributed to the increase in AgNB's surface area. In the cases of *Escherichia coli*, *Pseudomonas aeruginosa*, and *Candida albicans* there is no big difference between AgNBs. This means that in spite of the increase in surface area of the nanoparticles, another factor retards the improvement of the antimicrobial activity, such as Ag. Since nanosilver has a large specific surface area, it effectively interacts with bacteria and

considerably slows down their growth (fig. 6) [40,41].

Samples	Treated sample		Reference*	
	Inhibition zone (mm)		CN	MIZ
	<i>A. donax</i> ext.	AgNPs of <i>A. donax</i>		
Test bacteria				
1 <i>Escherichia coli</i>	16	18	17	–
2 <i>Pseudomonas aeruginosa</i>	15	18	15	–
3 <i>Bacillus cereus</i>	11	16	13	–
4 <i>Staphylococcus aureus</i>	11	19	13	–
5 <i>Candida albicans</i>	19	22	–	11

Table [5]: Antimicrobial activity expressed as inhibition diameter zones in millimeters (mm) of chemical compounds against the pathological strains based on well diffusion assay.



Candida albicans *Escherichia coli* *Pseudomonas aeruginosa*



Bacillus cereus *Staphylococcus aureus*

Figure [6]: Inhibition zone diameter (millimeter) of the samples

Conclusion:

The spectrometric techniques of *A. donax* extract led to the isolation and identification of 16 natural flavonoid compounds. *A. donax* ethanolic extract possess high free radical scavenging activity than its nano extract and considered natural free radical scavenging agents.

While the nano extract of *A. donax* has greater antimicrobial activity against some bacteria and fungi as well as its cytotoxic effect on the cancer cell lines A-431 (skin cancer), PC3 (prostate cell line), HCT-116 (colon cell line), and BJ-1 (normal skin fibroblast) than its ethanolic extract.

References

- 1-Christenhusz, M. J. M. and Byng, J. W., The number of known plants species in the world and its annual increase. *Phytotaxa*, 261 (3): 201–217, 2016.
- 2-Harborne, J. B., and Williams C. A., Flavonoid patterns in leaves of the Gramineae. *Biochem Syst. Ecol.* 4, 267–280, 1976.
- 3- Boulos, L., Flora of Egypt, vol. 1 & 4. Al Hadara Publishing. (1999 & 2005) Cairo, Egypt.

- 4- Fahmy, A. G., Grasses in Ancient Egypt. *Kew Bull.* 62, 507–511, 2007.
5. Miles, D.H., Tunsuwan, K., Chittawong, V., Hedin, P.A., Kokpol, U., Ni, C.Z. and Clardy, J., Agrochemical activity and isolation of N-(bromophenyl)-2,2- diphenylacetanilide from the Thai plant *Arundodonax*. *J. Nat. Prod.*, (56)1590-1593 (1993).
6. Duke, J. A. and Wain, K. K., Medicinal plants of the world. Computer index with more than 85,000 entries. (3) 1981.
7. Passalacqua, N.G., Guarrera, P. M. and De Fine, G., Contribution to the knowledge of the folk plant medicine in Calabria region (Southern Italy). *Fitoterapia*, 78, 52-68, 2007.
- 8- Safa, O., Soltanipoor, M.A., Rastegar, S., Kazemi, M., Dehkordi, K.N. and Ghannadi, A., An ethnobotanical survey on hormozgan province, Iran. *Avicenna, Journal of Phytomedicine*, 3(1), 64-81, 2003.
- 9-Al-Snafi, A. E., The constituents and biological effects of arundo donax. a review, *international journal of phytopharmacy research*, 6, 34-40, 2015.
- 10- Zayed, M., Eisa, W., Abdel-Moneam, Y., Elkousy, S., Atia, A., Ziziphus spina-christi based bio-synthesis of Ag nanoparticles. *Journal of Industrial and Engineering Chemistry*, 23, 50–56, 2015.
- 11- Sun, T., Tang, J. and Powers, J.R., Effect of pectolytic enzyme preparations on the phenolic composition and antioxidant activity of asparagusjuice. *Journal of Agricultural and Food Chemistry*, 53(1), 42-48, 2005.
- 12.Shinji M , Yuichi Y , Mikari E , Haruhiko M , Akira M , Motohiro T, Takuma S , Antitumor activity of a novel orally effective nucleoside, 1-(2-deoxy-2-fluoro-4-thio- β -D-arabinofuranosyl) cytosine, *Cancer letters*, 129 (1), 103-110,1998.
- 13-Barry, A. L., Procedure for testing antimicrobial agent in agar media. In V. Lorianed) *Antibiotica in laboratory medicines*. Willims and Wilkins Co. Baltimore. 23(1)(1980).
- 14-Frey, F.M and Rayan, M., Antibacterial activity of traditional medicinal plants used by Haudenosaunee peoples of New York State, *BMC Complementary and Altrnative Medicine*. 64(10)(2010).
- 15- Hindler, J. A.; Howard, B. J. and Keiser, J.F., Antimicrobial agents and Susceptibility testing. *Clinical and pathogenic Microbiology*. Mosby-Year Book Inc., St. Louis, MO, USA(1994).
- 16- Kite, G. C., Veitch, N.C., Identification of common glycosyl groups of flavonoid O-glycosides by serial mass spectrometry of sodiated species. *Rapid Commun. Mass Spectrom.* 25, 2579-2590 (2011).
- 17- Zhuan-Hong, Li., Han Guo, Wen-Bin Xu, Juan Ge, Xin Li, MireguliAlimu, and Da-Jun He, Rapid Identification of Flavonoid Constituents Directly from PTP1B Inhibitive Extract of Raspberry (*Rubusidaeus L.*) Leaves by HPLC–ESI–QTOF–MS–MS. *J Chromatogr Sci.*, 54(5), 805–810, 2016.
- 18- Venkatalakshmi, P., Vadivel, V., Brindha, P., Identification of flavonoids in different parts of *minaliacatappa L.* Using LC-ESI-MS/MS and investigation of their anticancer effect in EAC cell line model. *Pharm.Sci.and Res*, 8, 176–83, 2016.
- 19- Fatma, S., Abd El -Aal, H. Sh., Mohammed, M. H. I., and Lotfy D., I., Chemical profiling of polyphenols in *Thunbergialata* and in silico virtualscreening of their antiviral activities against COVID-19. *Azhar Int J Pharm Med Sci.* 1 (2), 94–100, 2021.
- 20- Asmaa S. Abd Elkarim, Amal H. Ahmed, Hanan A.A. Taie, Abdelbaset M. Elgamal, Mohammed Abu-Elghait and Samah Shabana. *Synadeniumgrantii* Hook f.: HPLC/QTOF-MS/MS tentative identification of the phytoconstituents, antioxidant, antimicrobial and antibiofilm evaluation of the aerial parts *Rasayan J. Chem.*, 14(2), 811-828, 2021.
- 21- Jeevan, K., P., Kenneth, J., Marion, K., Landon, W., Michelle, S-J, Connie, W., Profiling and Quantification of Isoflavonoids in Kudzu Dietary Supplements by HPLC and EISI-TMS. *J. Agric. Food Chem.*, 51(15): 4213-18, 2003.
- 22- Rita, M., Micaela, M., S., Maria, C. Oliveira., Maria, J. M., Characterization of weld (*Reseda luteola L.*) and spurge flax (*Daphne gnidium L.*) by high-performance liquid chromatography–diode array detection–massspectrometry in Arraiolos historical textiles. *Journal of Chromatography.*, 1216, 1395–1402, 2009.
- 23- Waridel, P., Wolfender, J.-L., Ndjoko, K., Hobby, K.R., Major, H.J., Hostettmann, K., Evaluation of quadrupole time-of-flight tandem mass spectrometry and ion-trap multiple-stage

- mass spectrometry for the differentiation of C-glycosidic flavonoid isomers. *J. Chromatography*, 926, 29-41, 2001.
- 24-Yang, Y., Sun, X., Liu, J., Kang, L., Chen, S., Ma B, Quantitative and qualitative analysis of flavonoids and phenolic acids in snow chrysanthemum (*Coreopsis tinctoria*Nutt.) by HPLC/DAD and UPLC-ESI-QTOF-MS. *Molecules*, 21,1307, 2016.
- 25-Al Sayed, E., Martiskainen, O., Sinkkonen, J., Pihiaja, K., Ayoub, N., Singab, A. E., et al.,Chemical composition and bioactivity of *Pleiogyniumtimorense* (Anacardiaceae). *Natural Product Communications*, 5, 545–550, 2010.
- 26-Rita M, Micaela M. S, Maria C. O, Maria J. M, Characterization of weld (*Reseda luteola* L.) and spurge flax (*Daphne gnidium* L.) by high-performance liquid chromatography–diode array detection–mass spectrometry in Arraiolos historical textiles. *Journal of Chromatography*, 1216 1395–1402, 2009.
- 27-Ying-L, Ying SC,Liu X, HuangX Z Neng L M , XuSui M N ,Sheng W. Simultaneous determination of esculin and its metabolite esculetin in rat plasma by LC–ESI-MS_MS and its application in pharmacokinetic study, *J Chromatogr B Analyt Technol Biomed Life Sci* . 33, 907:27- 2012.
- 28-Kim, M.Y., Chung, I. M., Choi, D. C., and Park, H. J. Quantitative analysis of fustin and sulfuretin in the inner and outer heartwoods and stem bark of *Rhusvernificflua*. *Natural Product Sciences*, 15, 208–212, 2009.
- 29- Anghel B, Javier E. R , Carlos A , Beatriz S and Mario J. S, HPLC-UV-MS Profiles of Phenolic Compounds and Antioxidant Activity of Fruits from Three Citrus Species Consumed in Northern Chile. *Molecules*, 19, 17400-17421, 2014.
- 30-Unyong K b, Sang B H, Oh-Seung K, and Hye H Y. Identification of Phase I and Phase II Metabolites of Hesperetin in Rat Liver Microsomes by Liquid Chromatography-Electrospray Ionization-Tandem Mass Spectrometry. *Mass Spectrometry Letters*, 275-280, 2011.
- 31-Rivero, P., Goicoechea J, Urrutia A, Arregui F. Effect of both protective and reducing agents in the synthesis of multicolor silver nanoparticles. *Nanoscale Research Letters*, 8, 101-109, 2013.
- 32- Rai, M., Yadav, A., Plants as potential synthesiser of precious metal nanoparticles. progress and prospects. *IET Nanobiotechnol*, 7, 117-124, 2013.
- 33-Thakkar, K.N., Mhatre, S.S., Parikh, R.Y., Biological synthesis of metallic nanoparticles. *Nanomedicine*, 6, 257-262, 2010.
- 34-Samfira, I., Rodino, S., Petrache, P., Cristina, R.T., Butu, M., Butnariu, M., Characterization And Identity Confirmation Of Essential Oils By Mid Infrared Absorption Spectrophotometry. *DIGEST journal of nanomaterials and biostructures*. 10 (2), 557-565, 2015.
- 35-Butnariu, M.V., Giuchici, C.V., The use of some nano emulsions based on aqueous propolis and lycopene extract in the skin's protective mechanisms against UVA radiation. *Journal of nanobiotechnology*, 9(1):3-8, 2011.
- 36- Iravani S, Zolfaghari B. Green Synthesis of Silver Nanoparticles Using Pinuseldarica Bark Extract. *Biomed Res Int*, 2013,1-5, 2013.
- 37- Al-Snafi AE. The constituents and biological effects of Arundodonax - A review. *International Journal of Phytopharmacy Research*, 6(1): 34-40, 2015.
- 38- Park, J., Gim, S. Y. , Jeon, J.Y. , Kim, M. J. , Choi, H.K, and Lee, J. Chemical profiles and antioxidant properties of roasted rice hull extracts in bulk oil and oil-in-water emulsion. *Food Chemistry*, 272, 242–250, 2019.
- 39- Parker, T. D. , Adams, D. , Zhou, K. , Harris, M. , & Yu, L. Fatty acid composition and oxidative stability of cold-pressed edible seed oils. *Journal of Food Science*, 68(4), 1240–1243, 2003.
- 40- Leporatti ML and Impieri M. Ethnobotanical notes about some uses of medicinal plants in Alto TirrenoCosentino area (Calabria, Southern Italy). *Journal of Ethnobiology and Ethnomedicine*, 3: 34-39, 2009.
- 41- Wang L, Hu C, and Shao L. The antimicrobial activity of nanoparticles: present situation and prospects for the future. *Int J Nanomedicine*, 12: 1227–1249, 2017.